Evaluation of Television Infrared Observation Satellite (TIROS-N) Operational Vertical Sounder (TOVS) spaceborne CO_2 estimates using model simulations and aircraft data

Philippe Peylin, Francois-Marie Breon, Soumia Serrar, Yogesh Tiwari, Alain Chedin, Manuel Gloor, Takashi Machida, Carl Brenninkmeijer, Andreas Zahn, Philippe Ciais

Evaluation of Television Infrared Observation Satellite (TIROS-N) Operational Vertical Sounder (TOVS) spaceborne CO_2 estimates using model simulations and aircraft data

Philippe Peylin,[1] Francois Marie Bréon,[2] Soumia Serrar,[2,3] Yogesh Tiwari,[4,5] Alain Chédin,[6] Manuel Gloor,[7] T. Machida,[8] C. Brenninkmeijer,[9] Andreas Zahn,[10] and Philippe Ciais[2]

Received 21 December 2005; revised 21 November 2006; accepted 24 November 2006; published 15 May 2007.

[1] CO_2 mixing ratio derived from spaceborne measurements of the Television Infrared Observation Satellite (TIROS-N) Operational Vertical Sounder (TOVS) instrument onboard NOAA-10 available for the time period 1987–1991 are evaluated against modeling results and aircraft measurements. The model simulations are based on two transport models and two sets of surface fluxes which have been optimized in order to fit near-surface atmospheric CO_2 measurements through a transport model (using an inverse procedure). In the tropics the zonal mean annual cycle and growth rate of the satellite product are consistent with those of the models. However, north-to-south gradients and spatial distributions for a given month show large differences. There are large regional patterns that can reach 7 ppm in the satellite retrievals (over regions of a few thousand kilometers wide) but are absent in the model predictions. The root-mean-square (RMS) differences between the models and the satellite product are around 1.7 ppm. One time series of the model CO_2 trend is used to extrapolate to the airborne measurement periods (1991–2003) both the satellite and the model monthly products to the airborne measurement period. The RMS difference between the airborne measurements and the extrapolated model predictions is around 1 ppm, while it is 2 ppm for the satellite estimate. These comparisons suggest that the large spatial variability of TOVS retrievals reflects substantial regional biases and noise which need to be reduced before remotely sensed CO_2 from TOVS will help constrain our knowledge of the carbon cycle.

Citation: Peylin, P., F. M. Bréon, S. Serrar, Y. Tiwari, A. Chédin, M. Gloor, T. Machida, C. Brenninkmeijer, A. Zahn, and P. Ciais (2007), Evaluation of Television Infrared Observation Satellite (TIROS-N) Operational Vertical Sounder (TOVS) spaceborne CO_2 estimates using model simulations and aircraft data, *J. Geophys. Res.*, *112*, D09313, doi:10.1029/2005JD007018.

1. Introduction

[2] Determining the spatial and temporal structure of surface carbon fluxes has become a major scientific, but also political, issue during the last decade. In the so-called ''bottom up'' approach, sparse observations of surface fluxes are up-scaled in space and time with biogeochemical models. In the so-called ''top down'' or ''inverse'' approach, observed atmospheric concentration gradients are used to unravel surface fluxes, given some description of the atmospheric transport. This approach has been widely used to invert concentration measurements from global surface networks [*GLOBALVIEW-CO_2*, 2005] to estimate the spatial distribution of annual mean surface fluxes [*Gurney et al.*, 2002; *Fan et al.*, 1998] and their interannual variability [*Baker et al.*, 2006; *Bousquet et al.*, 2001; *Rödenbeck et al.*, 2003].

[3] Major limitations of the inverse approach are the uncertainties in atmospheric transport mixing and the low density of atmospheric CO_2 concentration measurement network based on about 100 surface stations unevenly distributed over the world. With such network, key results have been obtained at the continental scale [*Gurney et al.*, 2002; *Bousquet et al.*, 2001] but the uncertainty in the retrieved surface fluxes on subcontinental (or regional) scales is still too large both for monitoring purposes as well as for making progress in our understanding of the carbon cycle. As a consequence, the density of CO_2 in situ observations, including regular aircraft profiles, has increased in recent years. Another new perspective has arisen

[1]Laboratoire de Biogéochimie Isotopique, Thiverval-Grignon, France.
[2]Laboratoire des Sciences du Climat et de l'Environnement, Gif sur Yvette, France.
[3]Now at Research Department, Satellite Section, European Center for Medium Range Weather Forecasts, Reading, UK.
[4]Max-Planck-Institut für Biogeochemie, Jena, Germany.
[5]Now at Indian Institute of Tropical Meteorology, Pune Maharashtra, India.
[6]Laboratoire de Météorologie Dynamique, Palaiseau, France.
[7]Earth and Biosphere Institute, University of Leeds, Leeds, UK.
[8]National Institute for Environmental Studies, Tsukuba, Japan.
[9]Max Planck Institute for Chemistry, Mainz, Germany.
[10]Institut for Meteorology and Climate Research (IMK), Eggenstein-Leopoldshafen, Germany.

0148-0227/07/2005JD007018

with the possibility to measure atmospheric CO_2 from space. Satellite-based observations of CO_2 have the potential to dramatically increase the spatial and temporal coverage of CO_2 measurements. On the other hand satellite products are vertically integrated concentrations rather than point-wise measurements which are more closely linked to the fluxes of interest. Several retrieval methods have been proposed to optimize the use of existing or forthcoming satellite observations. The first CO_2 estimate derived from spaceborne measurements was obtained using the Television Infrared Observation Satellite (TIROS-N) Operational Vertical Sounder (TOVS) [*Chédin et al.*, 2003]. Other similar products [*Engelen and McNally*, 2005; *Crevoisier et al.*, 2004] are based on data from the Atmospheric Infra-Red Sounder (AIRS) and the recent study of *Barkley et al.* [2006] on data from Sciamachy. The information content of the retrieved products is unclear at this stage. Validation of these satellite retrievals is therefore of interest both to see if these data can improve our current knowledge of the carbon cycle but also help design upcoming dedicated missions. Such missions include the Orbiting Carbon Observatory (OCO, [*Crisp et al.*, 2004]) and the Greenhouse gases Observing Satellite (GOSAT, Jaxa, http://www.jaxa.jp/missions/projects/sat/eos/gosat/index_e.html, 2006).

[4] The purpose of this paper is to assess the accuracy of the first satellite estimate of CO_2 concentration, retrieved from the TOVS instrument data for the period July 1987 to June 1991, in the tropical zone (20N–20S). A first qualitative evaluation of this product has been presented by *Chédin et al.* [2003] and focused on zonal means and on comparisons with upper tropospheric CO_2 measurements made on board commercial aircrafts over the western Pacific between 1993 and 1999 [*Matsueda et al.*, 2002]. Another CO_2 product derived from TOVS measurements, the so called Night minus Day Difference (NDD) has been proposed by *Chédin et al.* [2005] as a proxy for the biomass burning activity. We do not consider this new product but rather extend the initial validation of monthly CO_2 fields by comparing TOVS retrievals with simulations of the full three-dimensional CO_2 field based on two different model simulations. We also include in the analysis comparisons with aircraft measurements other than the *Matsueda et al.* [2002] data that so far have not been used to assess CO_2 retrievals from space. The model simulations rely on two different transport models, TM3 and LMDz, and two different sets of surface fluxes previously optimized toward surfaces atmospheric observations through an inverse procedure. The use of two different models with different estimates of the surface fluxes provides a rough indication of the current uncertainties in the atmospheric concentration in the upper troposphere. The aircraft data provide in situ "truth" although over a limited spatial and temporal scale and a different time period than TOVS retrievals. These data will be used for a "climatological" comparison of broad general patterns with TOVS and model data, ignoring the details of interannual variability.

[5] In the following, we first describe the model and data used for this validation exercise. We then compare the satellite and model CO_2 concentrations at different spatial and temporal scales. In section 4, we use airborne data to compare the accuracy of the model and satellite estimates. These comparisons are further used to discuss the performance of the TOVS CO_2 estimates.

2. Data Description

2.1. Satellite Estimates

[6] The retrievals analysed here are derived from a retrieval method proposed and applied to TOVS data by *Chédin et al.* [2003]. The main mission of TOVS is to measure atmospheric temperature and moisture profiles at the global scale. The National Oceanic and Atmospheric Administration (NOAA) polar meteorological satellite series has provided continuous observation of the Earth atmosphere and surface since 1978 [*Smith et al.*, 1979]. This series of satellites carry TOVS, which is a multisensor package, composed of the High-resolution Infrared Radiation Sounder (HIRS-2), the Microwave Sounding Unit (MSU) and the Stratospheric Sounding Unit (SSU). In the 15 μm and 4.3 μm spectral bands, HIRS radiances depend mostly on the atmospheric temperature profile along the view of sight but also on the CO_2 concentration as well as the concentrations of other greenhouse gases (O_3 around 15 μm, N_2O and CO around 4.3 μm) [*Chédin et al.*, 2002]. The observations made simultaneously by MSU in the oxygen microwave absorption band, also strongly depend on temperature, but are neither sensitive to CO_2, nor to other greenhouse gases. Thus the combination of MSU and HIRS data permits in principle to differentiate between the temperature and CO_2 concentration signatures in the HIRS radiances.

[7] The approach developed by *Chédin et al.* [2003] is based on a nonlinear regression (neural network) technique. The neural network was trained with the results from radiative transfer simulations for a large set of representative atmosphere profiles. It was then applied to radiances observed on NOAA-10, between July 1987 and June 1991, in the tropical zone (30N–30S). Higher-quality retrievals are expected in the tropical area compared to the extratropics because of the relatively high tropopause height and low variability of the temperature profiles. There is the potential for an extension of the method to data from other NOAA satellites, which would provide a time series covering a period of more than 20 years. The retrieval algorithm described by *Chédin et al.* [2003] underwent some improvements which led to a significant reduction in the magnitude of the retrieved regional CO_2 gradients, as described by *Chédin et al.* [2005].

[8] Individual cloud-free retrievals were binned into monthly fields at a spatial resolution of $1^\circ \times 1^\circ$ and then smoothed with a boxcar averaging procedure with $15^\circ \times 15^\circ$ resolution and restricted to the 20S–20N latitude band, in full compliance with the procedure described by *Chédin et al.* [2005]. Such averaging appeared necessary to smooth the large noise observed with the individual retrievals. To compare the satellite product to model simulations, it is necessary to properly take into account the vertical weighting function of the retrieval algorithm. The weighting function was determined through radiative transfer simulations based on the atmospheric profiles of the Thermodynamic Initial Guess Retrieval (TIGR) database [*Chédin et al.*, 1985; *Chevallier et al.*, 1998]. A uniform perturbation of CO_2 mixing ratio was applied sequentially to each of the 40 layers (i) of the TIGR database. The perturbed atmospheric profiles were then used

as input to a radiative transfer model to simulate TOVS radiances. The neural network was then applied to these radiances to obtain the theoretical change of the column mean apparent mixing ratio ($q^{NeuralNet}$) given a mixing ratio perturbation $\delta q_i = \varepsilon$ ppm in layer i:

$$F_i = \frac{q^{NNet}(\delta q_i = \varepsilon) - q^{NNet}(\delta q_i = 0)}{\varepsilon} [\text{ppm/ppm}] \quad (1)$$

[9] In practice, in order to translate this vertical weighting function to the vertical discretization of each model, it is necessary to normalize for the TIGR layer thickness ΔP_i. Because F_i is not independent of the thickness (or equivalently the mass) of the TIGR layers, it is necessary to express F_i in units of δ (number of CO_2 moles in air column)/δ (number of CO_2 moles in layer i). This results in the quantity

$$G_i = \frac{\sum_l \Delta p_l}{\Delta p_i} F_i = \frac{p_{surf}}{\Delta p_i} F_i (\text{mol/mol}) \quad (2)$$

[10] The 40 G_i values are independent of the layer thickness and they can be interpolated to any vertical layer distribution. Note that they are normalized so that the sum of the G_i, weighted by layer pressure thickness, is 1. There are 7 different sets of G_i depending on the satellite observation view angle. Figure 1 displays the vertical weighting function derived from this procedure for nadir viewing. Because 80% of the CO_2 concentration sensitivity is between 90 and 440 hPa, the TOVS measurement processed through the neural network is only sensitive to the upper troposphere concentration. It is not sensitive to the boundary layer mixing ratio.

2.2. Model Simulations

[11] We performed two simulations of atmospheric CO_2 concentration for the period 1987–1991, using the LMDz and the TM3 transport models. Differences between the transport models include analyzed wind fields, parameterizations of subgrid-scale processes and the numerical methods used to solve the advection equation. The transport models are forced with carbon fluxes as boundary conditions. These have been previously estimated by inversions of atmospheric transport that use surface concentrations as input. Because the data used are mainly from the surface, one expects that these model simulations represent the lower-troposphere concentrations fairly well [*Peylin et al.*, 2005; *Rödenbeck et al.*, 2003].

[12] The LMDz simulation uses the general circulation model of the Laboratoire de Météorologie Dynamique, LMDz [*Sadourny and Laval*, 1984] with a spatial resolution of 3.75° × 2.5° longitude by latitude with 19 vertical levels. Although the model computes its own dynamics and mass transport, the simulated winds and temperature are nudged toward the analyzed fields of ECMWF with a time constant of 2.5 hours. We use the proper winds for each year of the simulation, starting in 1985 to allow for a two years spin-up period. Large-scale advection of trace species follows the Eulerian framework described by *Hourdin and Armengaud* [1999]. Deep convection is parameterized according to *Tiedtke* [1989] and the turbulent mixing in the boundary layer is based on the work of *Laval et al.* [1981]. The optimized CO_2 fluxes are taken from *Peylin et al.* [2005] inverse study. They are based on 15 years of atmospheric near surface CO_2 observations from a network of 76 stations.

[13] The horizontal resolution of the TM3 model [*Heimann and Körner*, 2003] is 4° × 5° latitude by longitude with 19 sigma-coordinate vertical layers. Transport in TM3 is driven by meteorological fields derived from the NCEP (National Center for Environmental Prediction) reanalysis [*Kalnay et al.*, 1996]. Tracer advection is calculated using the slopes scheme of *Russell and Lerner* [1981]. Vertical transport due to convective clouds is computed using the cloud mass flux scheme of *Tiedtke* [1989] and turbulent vertical transport by the stability-dependent vertical diffusion scheme of *Louis* [1979]. The CO_2 surface fluxes used as boundary conditions in the TM3 simulations are from the *Rödenbeck et al.* [2003] atmospheric transport inversion study. They are based on 20 years of atmospheric near surface CO_2 flask data from the NOAA/CMDL station network and vary with monthly time step. The spatial resolution of the fluxes is 8° × 10° latitude by longitude.

[14] Significant differences between the two simulations can be expected both at the surface in regions that are poorly sampled and in the upper atmosphere. In the context of the present work, the differences between the two simulations provide a rough estimate of the uncertainty in the CO_2 concentration field. However, although they use two different meteorological fields (NCEP versus ECMWF), the two models have the same vertical convection scheme (and only slight differences in the vertical discretization (19 levels)) so that the model result difference probably underestimate this uncertainty. For the comparison between the model results and the satellite data, we paid particular attention to potential sampling errors. The models outputs were sampled colocated in space and time with the TOVS measurements (nearest grid point). The model vertical profiles were averaged with the weighting function described above, accounting for the satellite viewing angle. The model results extracted with this procedure were then averaged to monthly means and smoothed spatially (15° × 15°) with the exact same procedure as the satellite data.

2.3. Airborne Campaigns

[15] Although sparse in time and space, in situ aircraft measurements are useful to evaluate both TOVS-CO_2 retrievals and model simulations. We use available measurements from regular programs of atmospheric observations or from several short-term research campaigns that were not designed to study atmospheric CO_2. We only consider here the data that cover the tropics and extend from the mid to the upper troposphere (from 5 to 12 km above ground). Table 1 gives the period, location, and references for each of these campaigns. The resulting set of data covers an altitude range that corresponds to the lower half of the satellite product vertical weighting function. CO_2 mixing ratio were measured either continuously or from flask sample using different sensors (see *Anderson et al.* [1996] for all PEM campaigns) with potential intercalibration differences. However, theses differences remain small (usually much less than 1 ppm) and they do not affect the spatiotemporal gradient measured within each campaign.

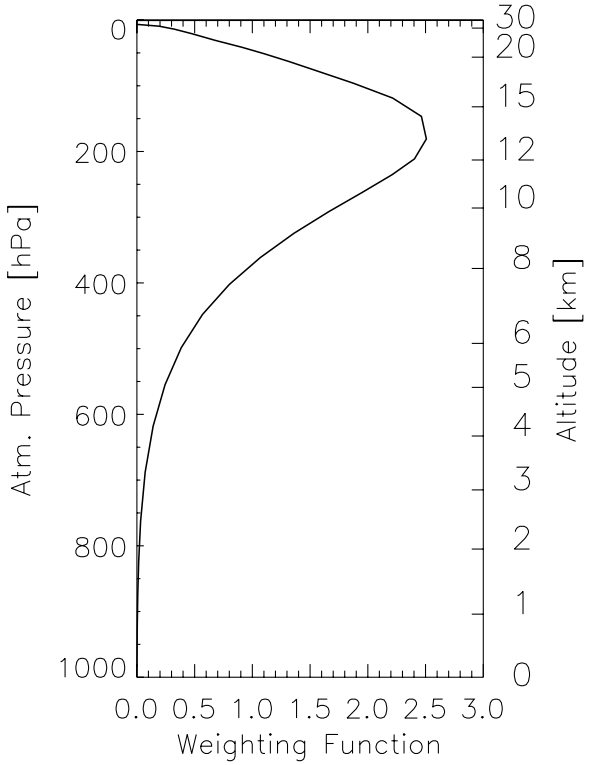

Figure 1. Vertical weighting function of Television Infrared Observation Satellite (TIROS-N) Operational Vertical Sounder (TOVS) (as implemented in LMDz and TM3) as a function of altitude.

[16] Most airborne data used in this study were collected several years after the satellite measurements used here. For the purpose of this comparison we therefore had to apply a time extrapolation method of the satellite data to the period of in situ measurements (see section 4). Such procedure is only intended to compare measurements from different years in a "climatological" sense (i.e., with the interannual growth rate removed). Note that the spatial coverage of the campaigns is biased toward the Pacific. Only few flights (CARIBIC campaigns) with CO_2 measurements exist over continental landmasses (see Figure 2).

3. Comparison Between TOVS and Model Estimates of Atmospheric CO_2

3.1. Zonal Means

[17] Figure 3 compares the time evolution (from June 1987 to July 1991) of the three different fields (TOVS, LMDz, and TM3) for 5 degrees zonal means from 20N to 20S. At first sight, the trend and seasonal cycles appear rather similar for the three products, especially in the Northern Hemisphere where the CO_2 signal is larger than in the south. The main cycles are in phase and with similar amplitude for the three curves. On the other hand, the model time series vary smoothly in time while TOVS shows large month-to-month fluctuations (up to 2 ppm) with strong interannual variations. In the Southern Hemisphere, the two simulations produce a much weaker seasonal cycle than in the Northern Hemisphere, while TOVS depicts large variations but with no clear seasonal cycle. Note that high-altitude in situ measurements from *Matsueda et al.* [2002] show a complicated seasonal cycle with two maxima, one around June–July and one around November–December. In order to quantify the differences between the three time series, we computed the amplitude of the seasonal cycles (decomposing each time series into its trend and seasonal component with the curve fitting procedure of *Thoning et al.* [1989]) and the root-mean-square value (RMS) of the pair differences, for each zonal band (Table 2).

[18] In the Northern Hemisphere, the large seasonal cycle of the land biosphere flux drives the CO_2 concentration in the boundary layer, which then propagates under attenuation into the upper troposphere. This results in a cycle with a maximum concentration in spring, and amplitude on the order of 4 ppm (Table 2). The land biosphere signal is much weaker in the Southern Hemisphere and surface stations there record a seasonal cycle that is only around 1 ppm [*Conway et al.*, 1988]. Other factors also have a noticeable impact. In particular, the Northern Hemisphere seasonal cycle influences that of the south through atmospheric transport across the Inter Tropical Convergence Zone.

Table 1. Aircraft Campaign Used to Compare With Model Simulations and Television Infrared Observation Satellite (TIROS-N) Operational Vertical Sounder (TOVS) Estimates[a]

Mission/Reference	Period	Location	Frequency
	Specific Campaigns		
PEM-WESTA [*Newell at al.*, 1996]	10 Sep 1991	northwestern Pacific	15 flights (1 s)
PEM-WESTB [*Hoell et al.*, 1997]	3 Feb 1994	northwestern Pacific	14 flights (1 s)
PEM-TA [*Hoell et al.*, 1999]	10 Aug 1996	tropical Pacific	34 flights (1 s)
PEM-TB [*Raper et al.*, 2001]	4 Mar 1999	tropical Pacific	36 flights (1 s)
TRACE-A [*Andreae et al.*, 1994]	10 Sep 1992	Brazil, South Atlantic, SW Africa	18 flights (1 s)
TRACE-P [*Jacob et al.*, 1996]	4 Feb 2001	northwestern Pacific	38 flights (1 s)
BIBLE-A [*Machida et al.*, 2002]	10 Sep 1998	western Pacific	14 flights (1 min)
BIBLE-B[b]	9 Aug 1999	western Pacific	12 flights (1 min)
BIBLE-C[b]	12 Nov 2000	western Pacific	16 flights (1 min)
	Regular Aircraft Observations		
JAL [*Matsueda et al.*, 2002]	1993–2003	north Australia to Japan	weekly flights (30 min)
CARIBIC [*Brenninkmeijer et al.*, 1999]	1997–2001	south India/Africa to Germany	32 flights (~30 min)

[a]The period between measurements is indicated in parenthesis.
[b]See http://www.eorc.nasda.go.jp/AtmChem/GLACE/bible/BIBLE.html for details.

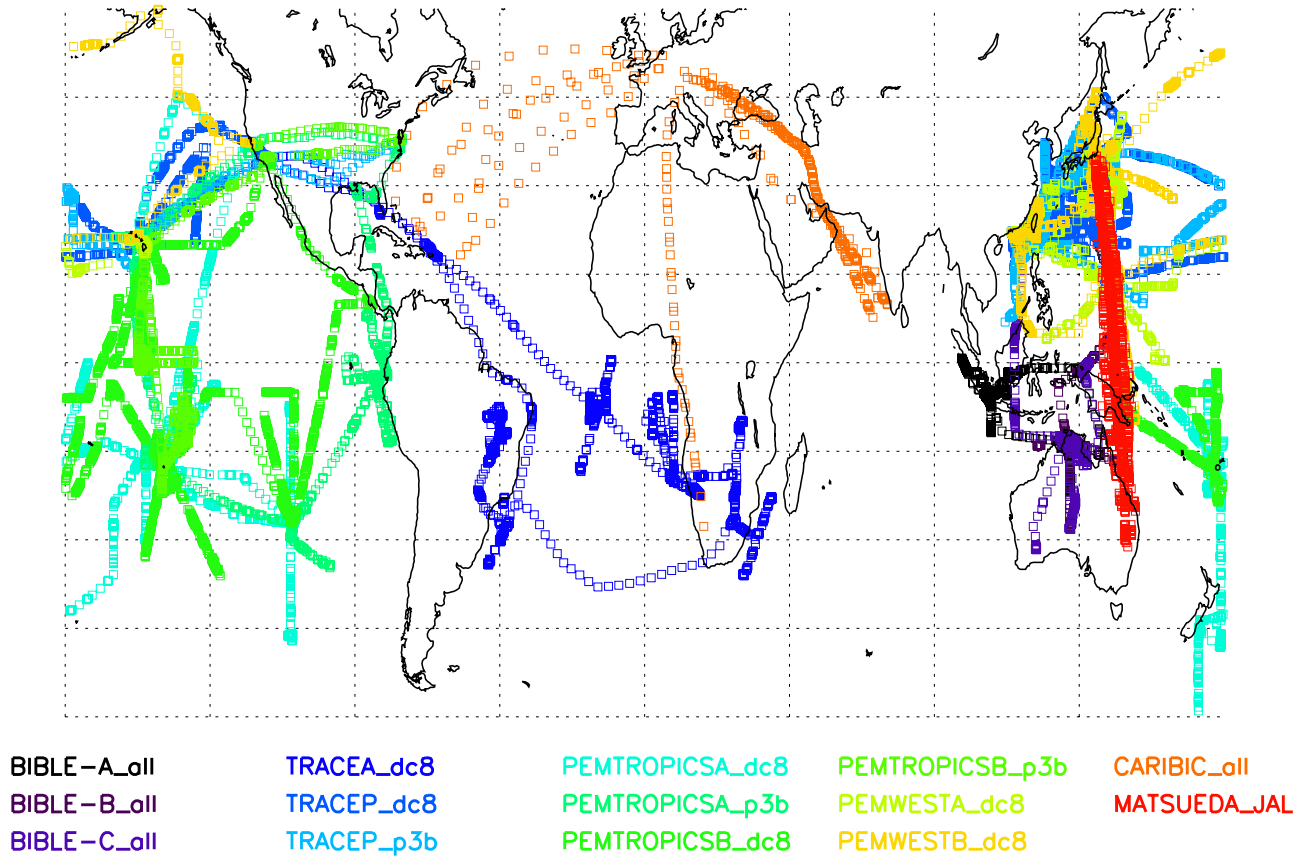

Figure 2. Spatial distribution of the airborne measurements used in the paper.

Studies with other tracers like SF_6 show relatively good agreement between model and data inter hemispheric gradients. These results make the large monthly excursions of TOVS in the Southern Hemisphere compared to the models appear truly suspect. The amplitudes of the seasonal cycles only significantly differ between the two models in the southern tropics (up to 20%), a situation corroborated by the RMS of the model differences that increase from north to south (Table 2). The magnitude of these model-to-satellite and model-to-model differences will be further analyzed when we will discuss the uncertainty of TOVS retrievals (section 5).

[19] We now consider in Figure 4 the annual cycle of latitudinal monthly mean north-to-south gradients for the three data sets averaged over the four years analyzed here. While the two models show similar gradients, the one from the satellite data is very different, in particular for June–August, October and November. The large difference with the model results, and the strong excursions (~0.5 ppm around 10° north or south), which cannot be easily linked to some physical processes, tend to indicate a problem with the satellite product. The large variations observed on a monthly basis tend to cancel out when averaged so that the yearly mean TOVS gradient is roughly similar to the model predictions.

3.2. Regional Patterns

[20] We now analyze the spatial patterns of the monthly mean CO_2 column weighted concentrations, with monthly mean subtracted (and a spatial smoothing of 15° × 15° longitude by latitude area). These patterns are shown in Figures 5a and 5b. The white zones on the maps correspond to areas with less than 275 satellite measurements per grid cell and month. Only the year 1990 is shown, as interannual variations for both model and satellite data are small compared with the difference between the satellite and model results. For example, the standard deviation of the differences between TOVS monthly data for 1990 and the monthly mean over the entire period (1987–1991) is two times smaller than the standard deviation of the satellite to model differences (~0.9 versus 1.8 ppm). The range of the color scales has been limited such that 90 % of the data is covered. There are some large and unexpected spatial structures in the TOVS retrievals. The range of the estimated values, on a monthly timescale, is close to 7 ppm, a value much larger than that of the models (~ 1.7 ppm). In addition, most of the gradients in the model are zonal, while the satellite product also varies strongly by latitude. As a consequence, not only the magnitude of the structures but also the spatial patterns is different.

[21] During the first half of the year, both model simulations exhibit a distinct zonality with CO_2 concentrations decreasing from north to south. This latitudinal gradient increases from January to May (see Figure 5a) and starts to decrease in June. It results from the interplay of anthropogenic emissions which mainly originate from the northern extratropics and the seasonal cycle of biospheric CO_2 uptake and release. TOVS retrievals do not show the same zonal structure. east-west variations are of the same mag-

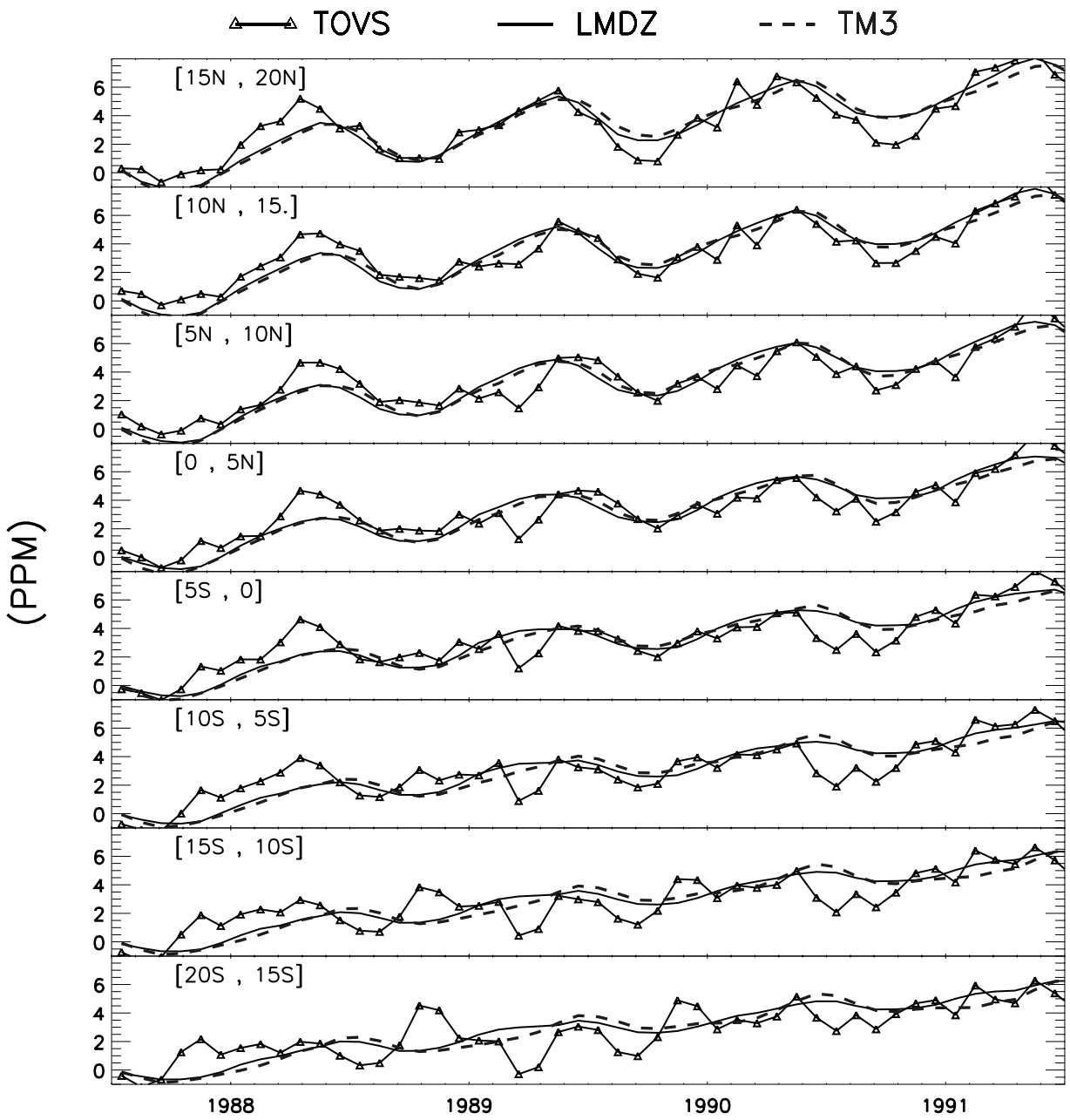

Figure 3. Time evolution of the zonal mean mixing ratios for the two models (LMDz and TM3) and TOVS data for different latitude bands (5° bands).

nitude as north-south variations. The origin of the longitudinal variations, partly associated to land sea contrast, is unclear. We have not been able to relate them to known biogeochemical or anthropogenic surface flux patterns, nor to characteristics of atmospheric transport. They are therefore rather suspicious especially since the vertical weighting function of the CO_2 concentration is significant in the mid to upper troposphere only, where gradients caused by surface fluxes are expected to be diluted by stirring and mixing in the atmosphere.

[22] The picture is slightly different for the model simulations during the second half of the year. During the boreal late spring and summer, the biospheric sink more than cancels the anthropogenic source to the atmosphere. As a consequence, the latitudinal gradient is much smaller than during previous months (see Figure 5b) and longitudinal variations emerge. Note that the patterns of these structures are not affected by the sampling of the model: monthly means based on a similar procedure but using all grid points rather than those observed by the satellite differ by less than 0.2 ppm. The monthly spatial patterns are somewhat different for the two models with differences up to 1 ppm. The most striking difference is observed in the Southern Hemisphere in October and November when LMDz shows a positive anomaly over Africa, while TM3 points to a local maximum over South America. These differences result from differences in the flux field that reflect our poor knowledge of the tropical CO_2 flux in particular over land

Table 2. Seasonal Cycle Amplitude TOVS-Data and Model Simulations for Different Latitude Bands, Together With the Root-Mean-Square (RMS) Value of the Differences Computed From the Zonal Mean Time Series of Figure 3[a]

Latitude Band	Seasonal Cycle Amplitude TOVS/LMDz/TM3	RMS of Differences TOVS-LMD/TOVS-TM3/LMD-TM3
15N–20N	4.80/3.46/3.26	0.92/1.08/0.31
10N–15N	4.31/3.28/3.17	0.86/0.89/0.31
5N–10N	3.88/2.89/2.91	0.99/0.95/0.29
0–5N	3.47/2.37/2.47	0.99/0.97/0.29
5S–0	3.13/1.87/2.01	1.02/1.06/0.30
10S–5S	2.86/1.48/1.78	1.14/1.23/0.33
15S–10S	2.46/1.30/1.61	1.34/1.24/0.36
20S–15S	2.69/1.19/1.48	1.34/1.39/0.38

[a]Seasonal cycle amplitude is given in ppm.

areas with biomass burning activity. This is due to a lack of ground stations in the tropics to constrain the surface fluxes with an inverse procedure. The TOVS patterns have an amplitude that is much larger and not significantly correlated with the prediction of any of the two models. Note that the nighttime minus daytime TOVS product (NDD) of *Chédin et al.* [2005], less sensitive to regional biases, is in favor of a larger biomass burning activity in Africa than in South America in 1990 and in particular for October and November, in agreement with the literature [see, e.g., *Duncan et al.*, 2003].

4. Statistical Comparison With Aircraft Measurements

[23] As just discussed, differences between satellite CO_2 estimates and the two model simulations are much larger than the difference between the two model results, and there is no obvious explanation based on missed surface fluxes or shortcomings in atmospheric transport modeling. A tempting explanation of the differences between the model and the satellite products is therefore that they are due to biases and noise in the latter.

[24] However, model simulations have so far only been validated at a few selected surface locations, while no similar effort has been made for the upper troposphere. There are potential causes for biases in the modeled fields, linked to uncertainties in the current parameterization of vertical convection and vertical diffusion in the models. Besides, surface fluxes are also poorly constrained in the tropical zone. Thus before jumping to conclusions the realism of high-altitude model transport needs to be assessed. For this purpose we rely here on a comparison with the airborne in situ measurements. The validation procedure implies the comparison of point data to vertically averaged, spatially smoothed, monthly mean fields, which is a potential cause for differences. As the resulting noise will be the same for the satellite and model fields, our conclusions will therefore not be affected by this problem.

[25] Because the satellite CO_2 product is available from July 1987 to June 1991, while the airborne campaigns happened all after September 1991, the two cannot be directly compared. However, given that the 1987–1990 TOVS retrievals present typical patterns each year, we may compare these patterns with the later aircraft data using a simple time extrapolation procedure. As time series of monthly mean upper troposphere CO_2 are dominated by the secular trend and the seasonal cycle, this can be achieved approximately in the following manner. A mean secular trend (smooth concentrations without the seasonal cycle, in ppm) expressed as function of year y, month m, $Tr(y, m)$ (computed with a polynomial fitted to the model raw data plus the residuals smoothed in time using a low pass filter in the spectral domain), is calculated for the upper troposphere tropical region sampled by TOVS for 1990 to 2003 on the basis of the LMDz simulation. When an in situ measurement is available for a given year y, month m, and location x (a given grid point), the concentrations from the satellite product and from the monthly column integrated model content for the year 1990 are extrapolated in time through:

$$C_{ext}[y, m, x] = C[1990, m, x] + Tr(y, m) - Tr(1990, m) \quad (3)$$

[26] The statistical differences between the airborne measurements and either the satellite product or the model simulations are summarized in Table 3 in terms of mean bias, and root-mean-square value (RMS) for each campaign. We choose the year 1990 as reference (largely unaffected by an El Niño event) but checked that the statistical results remain similar when using 1988 or 1989: the RMS differ by less than 0.1 ppm for TOVS (and less than 0.02 for the models). We also derive a global mean bias and RMS using all campaign data together. However, we subsampled uniformly the different campaigns in order to keep nearly the same number of measurements per unit of time and to give a similar weight to each of them. In addition the use of the TM3 model instead of LMDz to compute $Tr(y, m)$ as well as the degree of smoothing to derive such secular trend does not significantly change the results of Table 3. Finally, because many campaigns last less than a month and cover only a limited region, the statistical comparison with monthly satellite or model products should be interpreted with great care.

[27] The overall biases (last line in Table 3) are similar for the three estimates and relatively small, i.e., 0.3 ppm or less. On the other hand, the individual bias for each campaign can be much larger, up to 1 ppm for the models and 3 ppm for the satellite product. In general, the bias is larger (in absolute value) for the satellite product than for the models, with mean absolute values (and standard deviations) of 0.4 (0.3), 0.5 (0.3) and 1.1 (0.9) ppm for LMDz, TM3, and TOVS, respectively. The high standard deviation for TOVS also confirms the existence of unrealistically high regional biases. Remember, however, that for the short-period campaigns (lasting less than a month), there are few independent model or satellite estimates so that it is difficult to clearly distinguish bias and random error.

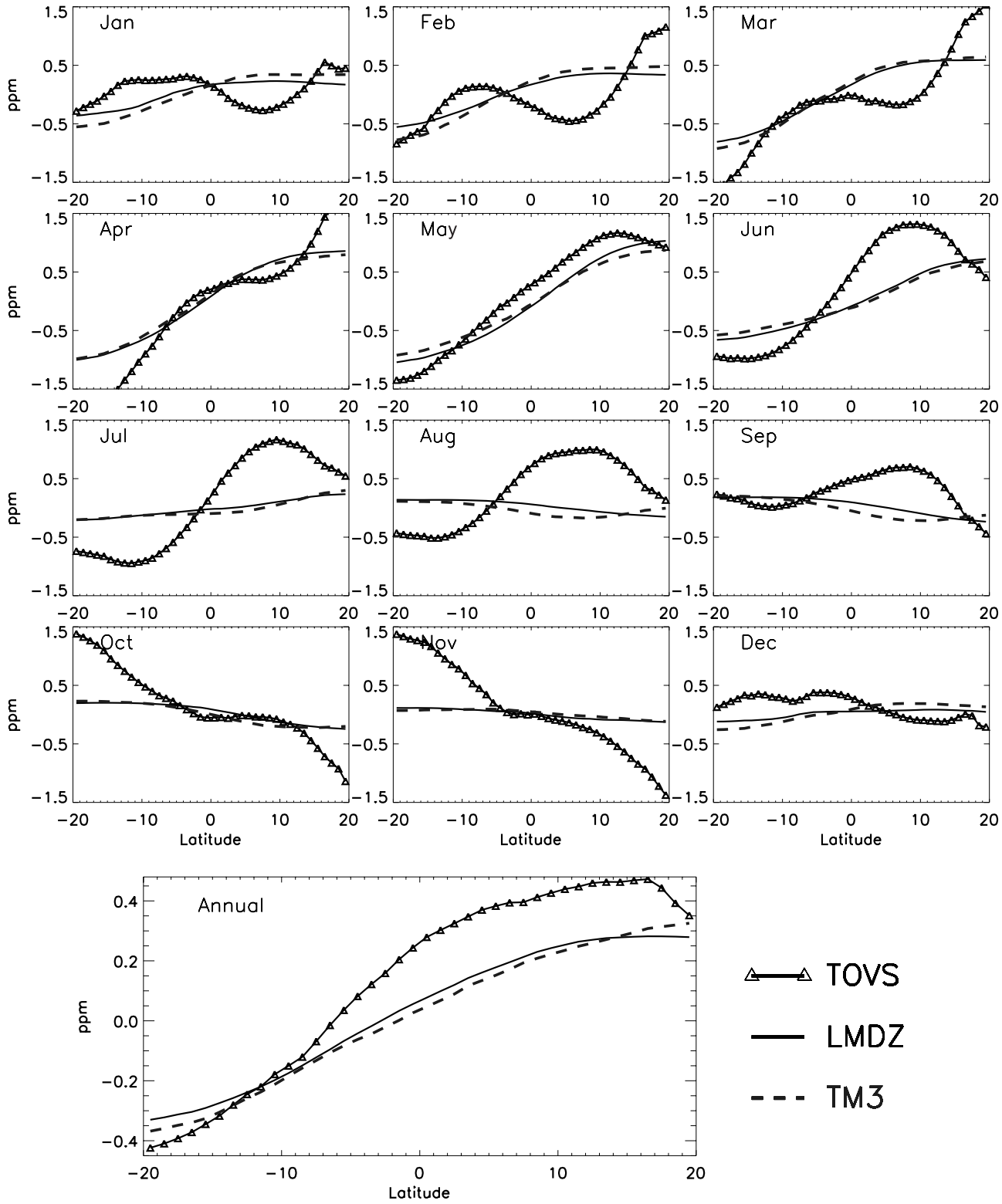

Figure 4. Monthly mean north-to-south mixing ratio gradients for the three estimates (TOVS and the two model simulations), averaged over the period July 1987 to June 1991. The annual mean gradient is also added.

[28] The RMS difference provides a complementary measure of the differences between the estimate and the true value. All campaigns combined, the RMS error is on the order of 1 ppm for the models, and 2 ppm for the satellite product. Campaign by campaign, the picture is rather similar; the two models behave similarly with typical RMS errors on the order of 1 ppm and differences in this parameter are less than 0.1 ppm, while the satellite product

Table 3. Summary of the Differences Between Model/TOVS Estimates and the In Situ Observations, Expressed in Terms of Mean Bias and Root-Mean-Square

	LMDz_integr		TM3_integr		TOVS	
	Bias	RMS	Bias	RMS	Bias	RMS
PEMTROPICSA	−0.08	0.49	−0.30	0.64	−1.40	1.98
PEMTROPICSB	0.25	0.92	0.18	0.97	0.61	1.41
PEMWESTA	0.77	1.26	0.84	1.32	0.83	1.32
PEMWESTB	−0.23	0.61	−0.55	0.75	0.61	1.31
TRACEA	−0.27	1.78	−0.70	1.85	1.62	2.40
TRACEP	−0.02	0.96	−0.54	1.07	−0.10	2.05
BIBLE-A	−0.71	0.95	−0.74	1.01	−0.38	1.02
BIBLE-B	−0.96	1.12	−1.05	1.21	−1.70	1.77
BIBLE-C	−0.66	0.81	−0.59	0.74	3.15	3.73
MATSUEDA	−0.08	0.83	0.01	0.88	0.30	1.88
CARIBIC	0.77	1.42	0.61	1.34	1.61	2.64
All campaigns	−0.10	0.96	−0.27	1.04	0.30	2.03

shows significantly larger RMS except for two campaigns, "PEMWESTA" and "BIBLE-A". Note that the statistical results for the "MATSUEDA" and "CARIBIC" campaigns are more robust as these campaigns cover several years.

[29] The typical value of 1 ppm for the RMS error for both model simulations is a rough indication of the model performance in the high troposphere of the tropics. Such a value is probably an overestimate of the modeling error as it includes the impact of temporal averaging and extrapolation and spatial smoothing. Similar statistics performed with the model simulations extracted at the exact space-time location of the airborne data (i.e., with no averaging, smoothing, and extrapolation) lead to values around 1 ppm and only slightly smaller than those of Table 3. Although the analysis of the actual performance of models in the upper troposphere is beyond the scope of this paper, such comparison indicates that the error from the extrapolation/smoothing procedure does not dominate the 1 ppm RMS error estimate.

[30] The 2 ppm RMS error for TOVS versus 1 ppm for the models suggests that the broad upper tropospheric patterns given by the models are closer to the truth than those from the satellite product. The difference between the monthly mean satellite product and the two model equivalents can be larger than 5 ppm locally (Figures 5a and 5b), while the RMS difference is on the order of 1.7 ppm in both cases with variations from 1.4 to 2.2 ppm depending on the months. These statistical results (satellite versus in situ data and satellite versus model simulations) indicate (1) that the RMS error of the satellite monthly mean product ($15^\circ \times 15^\circ$) is on the order of 2 ppm, (2) that the striking structures observed on TOVS retrievals (at a spatial scale of few thousand kilometers, Figures 5a and 5b) and not resolved by the model are suspicious and likely related to regional biases in the retrieval method, and (3) that these errors can be larger than 5 ppm. Further analysis is needed to explain the origin of these biases.

5. Discussion

[31] On the basis of our comparisons, the LMD TOVS CO_2 retrievals appear to capture the mean atmospheric CO_2 trend (around 1.5 ppm/year) and the predominance of a large seasonal cycle in the Northern Hemisphere (amplitude ~4 ppm), when averaged over large regions like 5 degree latitude bands. These results have been initially pointed out by *Chédin et al.* [2003] and also noted by *Chevallier et al.* [2005a]. They are encouraging as it is the first quantitative retrieval of atmospheric CO_2 concentration, and it is based on an instrument that was not designed for that purpose. However, an important question is whether these estimates can bring new information to the carbon cycle and, if so, at what spatial and temporal scales. To answer that question, we compare below an estimation of the accuracy that we currently need on atmospheric CO_2 mixing ratios to improve our knowledge of the atmospheric CO_2 variations to an evaluation of the noise in the satellite data.

[32] We propose successively two methods to estimate the accuracy needed, depending on the scale considered and on the basis of our model simulations. First, we simply use the "mean difference" between the two simulations used in this paper as an overall target. Second, we consider local features (in space and time) and define the accuracy need with either the largest concentration difference between the two simulations or an estimation of the local impact of a relatively "poorly constrained" process, such as biomass burning, using one atmospheric transport model.

[33] At monthly timescales, the two simulations show mostly similarities (Figures 5a and 5b) and the RMS of the differences is around 0.30 ppm over the year and range from 0.21 ppm in August to 0.39 ppm in May. Thus at the 15 degrees spatial scale the mean accuracy requirement (or signal to be detected) is on the order of 0.3 ppm. On the other hand, the RMS of the differences between TOVS and the two models are on the order of 1.7 ppm. Because such value results from large coherent spatial structures in TOVS that cannot be related to any known transport of biophysical process and because the validation to airborne samples has demonstrated a typical error of that magnitude, the 1.7 RMS value can be taken as an estimation of the noise in the current satellite retrieval. Such value is then roughly 6 times the required accuracy defined above.

[34] If we now consider the zonal means (5° zonal bands of Figure 3), the model-to-model RMS differences are around 0.30 ppm in the zonal bands north from the equator and around 0.35 to the south (Table 2). As before, we can use these values as a mean accuracy requirement for satellite data to reduce the uncertainty in zonal mean upper troposphere CO_2. On the other hand, the RMS differences between the satellite and model time series are close to 0.95 ppm in the north and 1.25 ppm in the south. If we assume again that this is mostly a result of noise of the satellite retrievals, one finds a ratio close to 3 between the noise and the signal for both hemispheres. The situation is thus more favorable at the zonal scale.

[35] At this point the variability (bias or noise) in the monthly TOVS product ($15^\circ \times 15^\circ$) appears prohibitive to provide valuable information on atmospheric CO_2 mixing ratio variations. This result has been confirmed by *Chevallier et al.* [2005a] in an attempt to estimate surface CO_2 fluxes from this data set. However, this result is a mean result based on the use of the whole data set. We will thus now briefly consider the same analysis using maximum absolute differences instead of mean RMS values and investigate the specific case of local (in space and time) biomass burning signals.

[36] At the regional scale (Figures 5a and 5b), the maximum model to model difference is on the order of

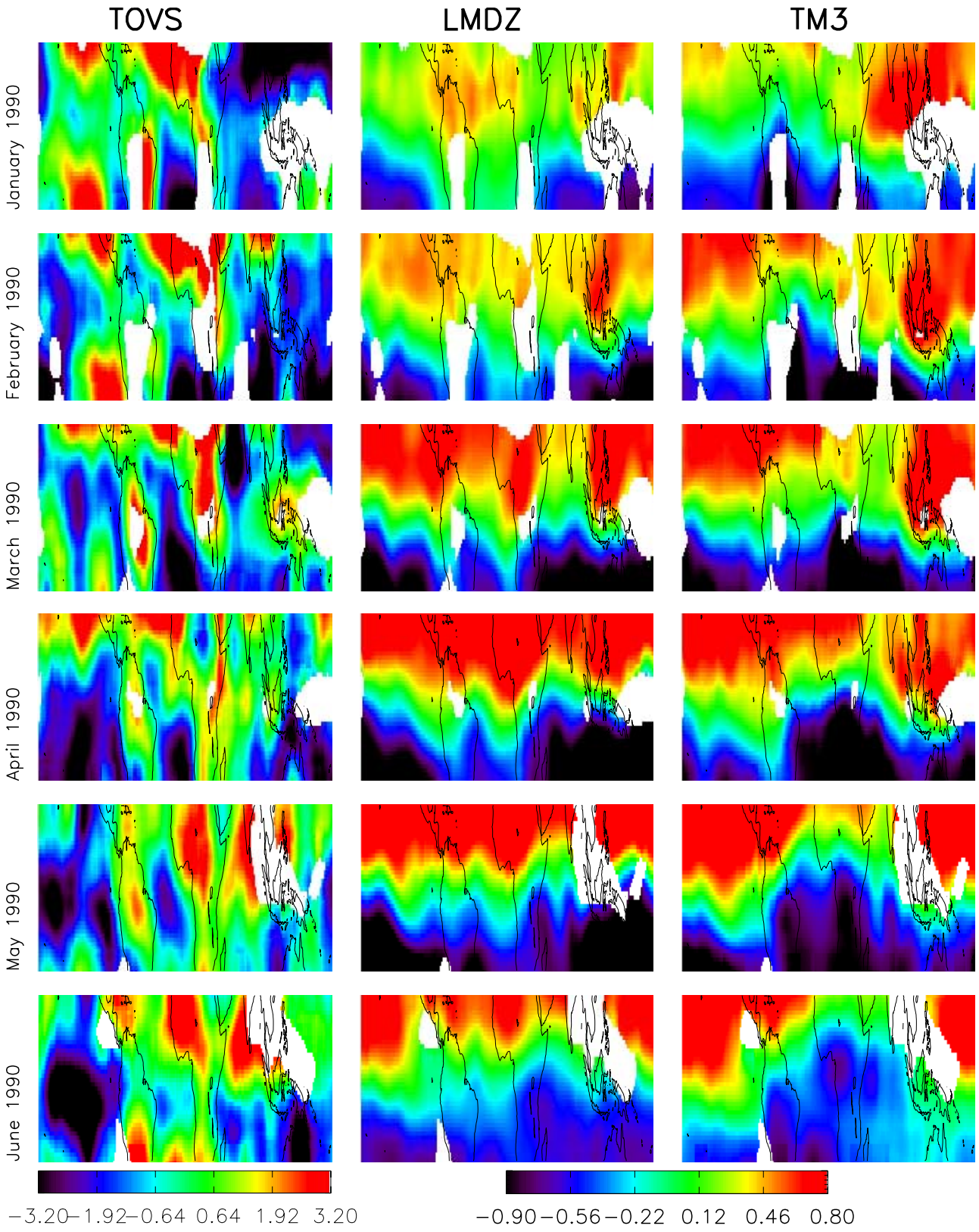

Figure 5a. Monthly CO_2 mixing ratio maps over the tropics for TOVS and LMDz and TM3 model simulations for January to June 1990. Mean values were subtracted from each map. We use two color tables, one for TOVS and one for both models, and adjust the range of the tables to truncate 5% of the minimum and maximum values.

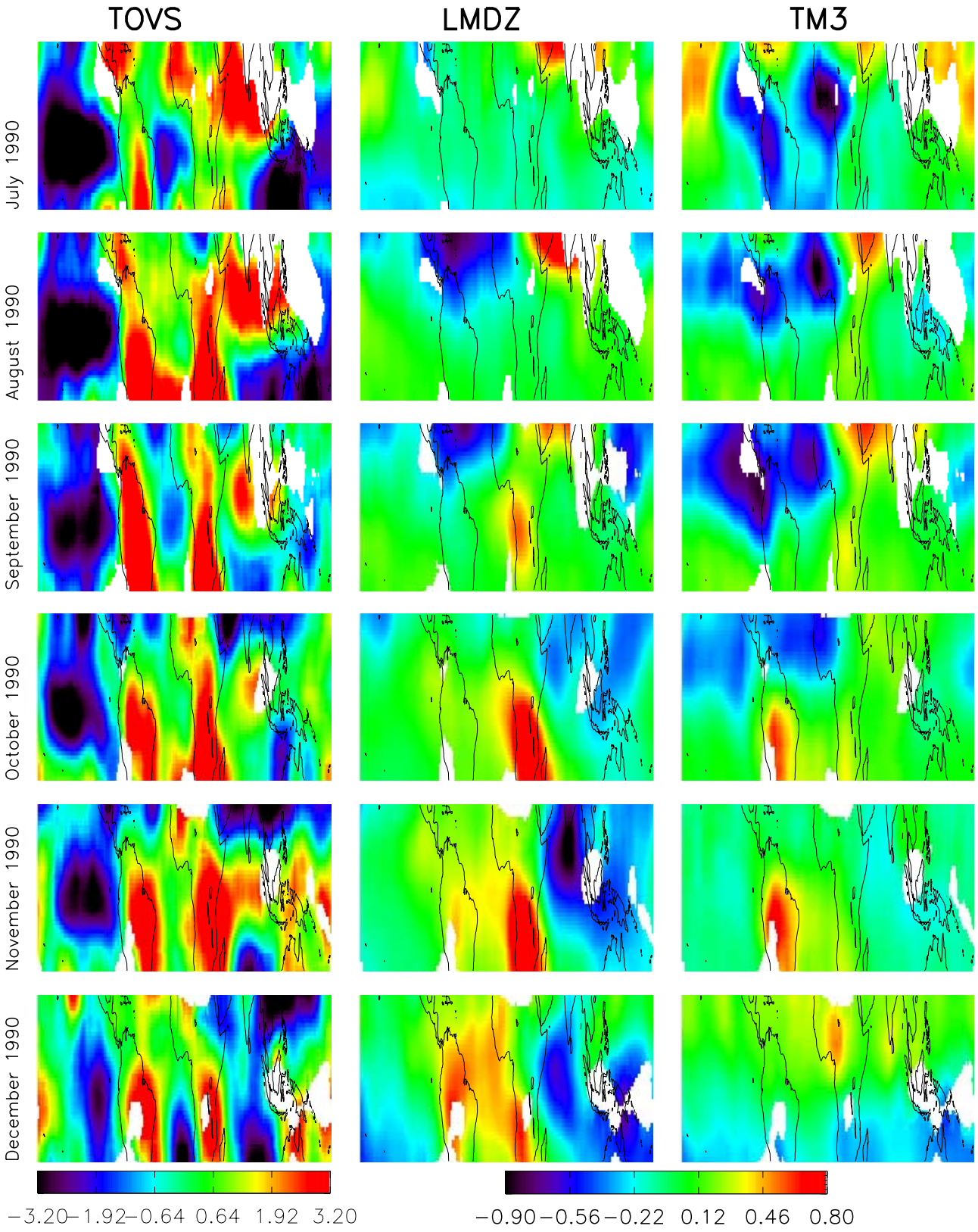

Figure 5b. Same as Figure 5a for July to December 1990.

1.4 ppm for few months, while the maximum satellite to model difference is around 6 ppm. This gives us a ratio between a need in accuracy and the satellite noise close to 4. At the zonal scale of Figure 3 the same approach based on maximum differences lead to similar ratio as with the RMS differences (~3), and the smallest value is only 2.4 for the [10N–15N] zonal band.

[37] Let us now consider biomass burning fluxes in the tropics, which are at present still poorly constrained. These events, intense and sporadic in nature, are a major source of uncertainty in the description of the surface CO_2 fluxes. We use an up-to-date estimate of the biomass burning CO_2 flux [*Van der Werf et al.*, 2003] that combines information on the space-time location of the fires (using space measurements) and on the amount of burned carbon (using CASA biogeochemical model [*Potter et al.*, 1993]). A monthly mean flux derived from the 1997–2001 period was transported by the LMDz model, using the 1990 meteorology. The resulting monthly mean CO_2 concentrations, processed consistently with the satellite measurements (spatiotemporal sampling, weighting function, smoothing procedures) are shown for few months with large tropical fires in Figure 6 (left). The impact on upper troposphere concentration is significant over several regions, up to about 1 ppm. This number gives an order of magnitude of the expected biomass burning signal, although this prediction critically depends on the amount of biomass that is burned, and on the representation of vertical mixing processes that may be specific over large fires. If we consider the monthly mean concentration at the lowest layer of the model (Figure 6, right), where the fluxes are injected, we clearly see different spatial patterns than when vertically averaged with TOVS function. For example, there are strong signals at the surface over Africa in June and July (Figure 6, right) that do not reach the upper troposphere and lower stratosphere in the LMDz simulation (Figure 6, left), i.e., altitudes around 10 km where TOVS vertical weighting function is significant. These differences highlight the strong influence of vertical mixing (especially deep convection) and vertical distribution of the injection (simply considered at the surface in our simulation) to simulate the contribution of local fire events to upper atmospheric CO_2 concentrations. The parameterizations of these processes are still rather uncertain in current transport models and further investigations need to be done.

[38] However, we can consider the surface concentration patterns in Figure 6 (around 3–5 ppm over large regions) as an upper limit of any vertically weighted average. The need in accuracy to clearly detect the upper troposphere CO_2 increase from biomass burning fluxes will thus be probably lower than 5 ppm (maximum surface signal in Figure 6) and on the order of 1 ppm (Figure 6, left). Such a value is still much lower than the estimated noise for TOVS CO_2 retrievals when using the maximum satellite to model difference (~6 ppm). However, the spatial patterns in Figure 6 from biomass burning are in good coherence with those of the NDD (nighttime minus daytime) TOVS retrievals, shown by *Chédin et al.* [2005]. This later product, much less sensitive to regional biases is more directly linked to the biomass burning events. The underlying hypothesis is that the signal of CO2 plumes is rapidly uplifted by fire-induced convection into the upper troposphere during the daytime peak of fire activity and then rapidly dispersed at night by large-scale atmospheric transport. It constitutes a potential promising source of additional information but a detail and rigorous comparison of that product with model simulations is beyond the scope of this paper.

[39] Overall our analysis of accuracy need versus noise/biases, although quite crude and only based on two model simulations, highlights the inability of the current TOVS retrievals to enhance our knowledge about the spatiotemporal variations of the atmospheric CO_2 mixing ratio. The errors in the satellite product are far from purely random as the patterns spread over spatial scales larger than the smoothing grid box of 15°. Besides, several coherent patterns are observed at the same place for several months in a row, or during the same month of several years (not shown). These consistent patterns likely result from signals other than CO_2 that produce regional biases in the current retrieval. The main causes for these regional biases are (1) errors in the forward radiative transfer model adjustment coefficients, calculated from comparisons between simulations using radiosondes (spatially poorly distributed, particularly over the tropics), and collocated satellite observations, (2) limitations in the representativeness of the regression training data set, and potentially (3) the ozone (and to a lesser extent water vapor) distributions that affect the TOVS channels used in the retrieval, because of their limited spectral resolution. More work remains to be done to properly assess the causes of these biases.

6. Summary and Conclusion

[40] In the work of *Chédin et al.* [2003, 2005], measurements from the TOVS instrument, onboard the NOAA-10 satellite, have been used to produce the first estimate of atmospheric CO_2 concentration from spaceborne observations. Although this instrument was never designed for that objective, this pioneering work has demonstrated that there is a CO_2 signature in the measured radiances. Indeed, the estimate of CO_2 concentration, derived using a nonlinear regression technique, reflect several well-known features such as the general growth rate of around 2 ppm per year, and the seasonal cycle of about 4 ppm in the Northern Hemisphere.

[41] On the other hand, global maps of retrieved CO_2 concentration show regional patterns that are unexpected. We have therefore evaluated the product against both model simulations and airborne measurements. These comparisons suggest that the satellite retrieved CO_2 concentration patterns, with an amplitude of several ppm, result mostly from biases but also noise in the method rather than being a real signal. Both comparisons with the modeling results and to in situ measurements suggest RMS errors of the TOVS monthly mean 15 × 15° product on the order of 2 ppm. These errors are not random as they extend over several thousands of km and have similar patterns from year to year. However, the nighttime (7.30 pm, local time) minus daytime (7.30 am, local time) difference (NDD) of TOVS retrievals [*Chédin et al.*, 2005], much less sensitive to these regional biases because of its differential character has been shown to be in coherence with the biomass burning activity at the regional level. It therefore constitutes a potential promising source of additional information.

[42] On the other hand, the two models investigated here show very consistent results with RMS differences of

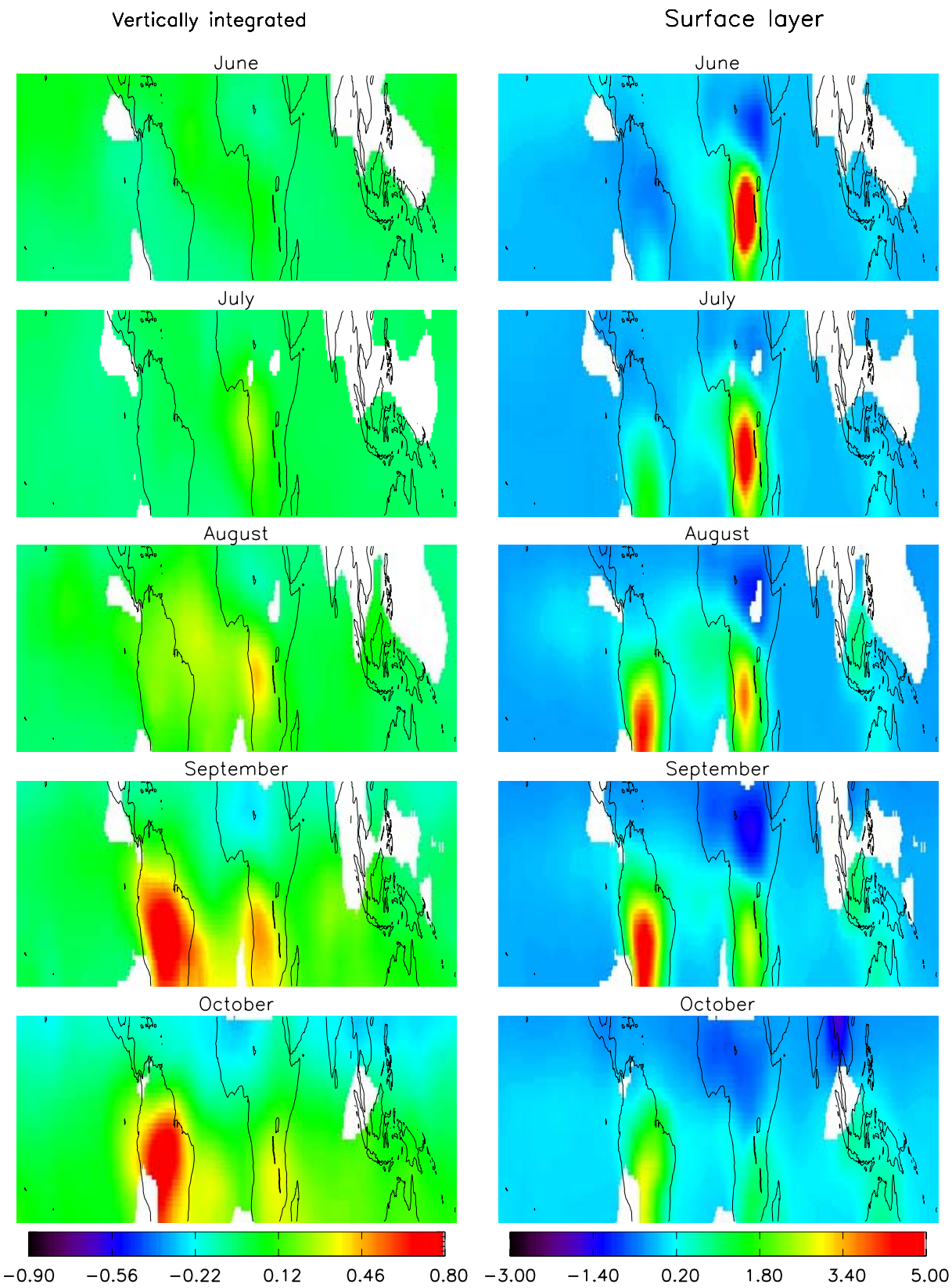

Figure 6. Monthly CO_2 mixing ratio maps of the biomass burning effect with the LMDz transport model (meteorology from 1990) and monthly mean sources from *Van der Werf et al.* [2003]. (left) Vertically integrated mixing ratio according to TOVS measurements (as in Figures 5a and 5b). (right) Surface layer mixing ratios. The sources correspond to a mean over the 1997–2001 period; they combine satellite observations and a model simulation (CASA). The mean mixing ratios for each month were subtracted from each map.

0.3 ppm, and a maximum RMS difference of 1.3 ppm over land areas with known biomass burning activity. The comparison of modeling results to airborne measurements shows an RMS difference on the order of 1 ppm. More upper air data, especially over the continents, would be very useful to assess more conclusively the performances of the models and a larger ensemble would also provide a better assessment of the current knowledge on upper air CO_2 concentration. On the basis of this limited set of airborne observation and model simulations, we have estimated that the error (mostly bias) in the TOVS monthly product is roughly 6 times the accuracy needed to improve our knowledge of the atmospheric CO_2 mixing ratio variations. Further developments thus require a strong improvement of our current understanding of the different sources of error. Note finally that recent CO_2 estimates from the AIRS satellite observations also reveal suspicious regional patterns when comparing with model simulations [*Tiwari et al.*, 2006].

[43] The typical 1 ppm model uncertainty (derived from model to aircraft comparison) is relevant in the context of accuracy requirements for future satellite CO_2 mission like OCO and GOSAT. It is a rough minimal requirement for accuracy and precision of monthly mean CO_2 estimates over scales of $10^\circ \times 10^\circ$ longitude by latitude. Any bias close or larger to 1 ppm would definitely hamper the use of these products (see for instance the analyses of *Chevallier et al.* [2005b] using AIRS data). However, if we consider regional events for restricted periods, those constraints might be slightly relaxed. Indeed, the ''synoptic'' or ''submonthly'' events can produce larger signals, which may be detected with a vertical weighting function that probes not only the upper but also the lower troposphere.

[44] **Acknowledgments.** This work was partly funded by the European COCO project: ''Measuring CO_2 from space exploiting planned missions 2001–2004''. This work was also supported by the BIBLE-C program at JAXA EORC, and the BIBLE-A and -B data were provided by the BIBLE archive at JAXA EORC. We would like to thank M. Heimann for fruitful discussions, and C. Rödenbeck and P. Bousquet for providing the surface fluxes for TM3 and LMDz, respectively.

References

Anderson, B. E., G. L. Gregory, J. E. Collins Jr., G. W. Sachse, T. J. Conway, and G. P. Whiting (1996), Airborne observations of spatial and temporal variability of tropospheric carbon dioxide, *J. Geophys. Res.*, *101*, 1985–1997.

Andreae, M. O., J. Fishman, M. Garstang, J. G. Goldammer, C. O. Justice, J. S. Levine, R. J. Scholes, B. J. Stocks, A. M. Thompson, B. van Wilgen, and the STARE/TRACE-A/SAFARI-92 Science Team (1994), Biomass burning in the global environment: First results from the IGAC/BIBEX field campaign STARE/TRACE-A/SAFARI-92, in *Global Atmospheric-Biospheric Chemistry*, edited by R. Prinn, pp. 83–101, Springer, New York.

Baker, D. F., et al. (2006), TransCom3 inversion intercomparison: Interannual variability of regional CO_2 sources and sinks, 1988–2003, *Global Biogeochem. Cycles*, *20*, GB1002, doi:10.1029/2004GB002439.

Barkley, M. P., M. P. Frieß, and P. S. Monks (2006), Measuring atmospheric CO_2 from space using Full Spectral Initiation (FSI) WFM-DOAS, *Atmos. Chem. Phys. Disc.*, *6*, 2765–2807.

Bousquet, P., P. Peylin, P. Ciais, C. Le Quere, P. Friedlingstein, and P. P. Tans (2001), Regional changes in carbon dioxide fluxes of land and oceans since 1980, *Science*, *290*, 1342–1346.

Brenninkmeijer, C. A. M., et al. (1999), CARIBIC–Civil aircraft for global measurement of trace gases and aerosols in the tropopause region, *J. Atmos. Oceanic Technol.*, *16*, 1373–1383.

Chédin, A., N. A. Scott, C. Wahiche, and P. Moulinier (1985), The improved Initialization Inversion method: A high resolution physical method for temperature retrievals from satellites of the TIROS-N series, *J. Clim. Appl. Meteorol.*, *24*, 128–143.

Chédin, A., S. Serrar, R. Armante, N. A. Scott, and A. Hollingsworth (2002), Signatures of annual and seasonal variations of CO_2 and other greenhouse gases from NOAA/TOVS observations and model simulations, *J. Clim.*, *15*, 95–116.

Chédin, A., S. Serrar, N. A. Scott, C. Crevoisier, and R. Armante (2003), First global measurement of midtropospheric CO_2 from NOAA polar satellites: Tropical zone, *J. Geophys. Res.*, *108*(D18), 4581, doi:10.1029/2003JD003439.

Chédin, A., S. Serrar, N. A. Scott, C. Pierangelo, and P. Ciais (2005), Impact of tropical biomass burning emissions on the diurnal cycle of upper tropospheric CO_2 retrieved from NOAA-10 satellite observations, *J. Geophys. Res.*, *110*, D11309, doi:10.1029/2004JD005540.

Chevallier, F., F. Cheruy, N. A. Scott, and A. Chédin (1998), A neural network approach for a fast and accurate computation of a longwave radiative budget, *J. Appl. Meteorol.*, *37*, 1385–1397.

Chevallier, F., M. Fisher, P. Peylin, S. Serrar, P. Bousquet, M. F-Bréon, A. Chédin, and P. Ciais (2005a), Inferring CO_2 sources and sinks from satellite observations: Method and application to TOVS data, *J. Geophys. Res.*, *110*, D24309, doi:10.1029/2005JD006390.

Chevallier, F., R. J. Engelen, and P. Peylin (2005b), The contribution of AIRS data to the estimation of CO_2 sources and sinks, *Geophys. Res. Lett.*, *32*, L23801, doi:10.1029/2005GL024229.

Conway, T., P. Tans, L. S. Waterman, K. W. Thoning, K. A. Masarie, and R. H. Gammon (1988), Atmospheric carbon dioxide measurements in the remote global troposphere, 1981–1984, *Tellus, Ser. B*, *40*, 81–115.

Crevoisier, C., S. Heilliette, A. Chédin, S. Serrar, R. Armante, and N. A. Scott (2004), Midtropospheric CO_2 concentration retrieval from AIRS observations in the tropics, *Geophys. Res. Lett.*, *31*, L17106, doi:10.1029/2004GL020141.

Crisp, D., et al. (2004), The Orbiting Carbon Observatory (OCO) Mission, *Adv. Space Res.*, *34*(4), 700–709.

Duncan, B. N., R. V. Martin, A. C. Staudt, R. Yevich, and J. A. Logan (2003), Interannual and seasonal variability of biomass burning emissions constrained by satellite observations, *J. Geophys. Res.*, *108*(D2), 4100, doi:10.1029/2002JD002378.

Engelen, R. J., and A. P. McNally (2005), Estimating atmospheric CO_2 from advanced infrared satellite radiances within an operational four-dimensional variational (4D-Var) data assimilation system: Results and validation, *J. Geophys. Res.*, *110*, D18305, doi:10.1029/2005JD005982.

Fan, S., M. Gloor, J. Mahlman, S. Pacala, J. Sarmiento, T. Takahashi, and P. Tans (1998), A large terrestrial carbon sink in North America implied by atmospheric and oceanic CO_2 data and models, *Science*, *282*, 442–446.

GLOBALVIEW-CO_2 (2005), *Cooperative Atmospheric Data Integration Project–Carbon Dioxide*, [CD-ROM], Natl. Oceanic Atmos. Administration, Clim. Monit. and Diagnostics Lab., Boulder, Colo. (Also available on Internet via anonymous FTP to ftp.cmdl.noaa.gov, Path: ccg/co2/GLOBALVIEW)

Gurney, K. R., et al. (2002), Towards robust regional estimates of CO_2 sources and sinks using atmospheric transport models, *Nature*, *415*, 626–630.

Heimann, M., and S. Körner (2003), *The Global Atmospheric Tracer Model TM3, Model Description and User's Manual, Release 3.8a*, Max-Planck Inst. for Biogeochem., Jena, Germany.

Hoell, J. M., D. D. Davis, S. C. Liu, R. E. Newell, H. Akimoto, R. J. McNeal, and R. J. Bendura (1997), The Pacific Exploratory Mission-West Phase B: February–March, 1994, *J. Geophys. Res.*, *102*, 28,223–28,240.

Hoell, J. M., D. D. Davis, D. J. Jacob, M. O. Rodgers, R. E. Newell, H. E. Fuelberg, R. J. McNeal, J. L. Raper, and R. J. Bendura (1999), Pacific Exploratory Mission in the tropical Pacific: PEM-Tropics A., August–September 1996, *J. Geophys. Res.*, *104*, 5567–5584.

Hourdin, F., and A. Armengaud (1999), Test of a hierarchy of finite-volume schemes for transport of trace species in an atmospheric general circulation model, *Mon. Weather Rev.*, *127*, 822–837.

Jacob, D. J., et al. (1996), Origin of ozone and NO_x in the tropical troposphere: A photochemical analysis of aircraft observations over the South Atlantic basin, *J. Geophys. Res.*, *101*, 24,235–24,250.

Kalnay, E., et al. (1996), The NCEP/NCAR 40-year reanalysis project, *Bull. Am. Meteorol. Soc.*, *77*, 437–471.

Laval, K., R. Sadourny, and Y. Serafini (1981), Land surface processes in a simplified general circulation model, *Geophys. Astrophys. Fluid Dyn.*, *17*, 129–150.

Louis, J. F. (1979), A parametric model of vertical eddy fluxes in the atmosphere, *Boundary Layer Meteorol.*, *17*, 187–202.

Machida, T., K. Kita, Y. Kondo, D. Blake, S. Kawakami, G. Inoue, and T. Ogawa (2002), Vertical and meridional distributions of the atmospheric CO_2 mixing ratio between northern midlatitudes and southern subtropics, *J. Geophys. Res.*, *107*, 8401, doi:10.1029/2001JD000910, [printed 108 (D3), 2003].

Matsueda, H., H. Y. Inoue, and M. Ishii (2002), Aircraft observation of carbon dioxide at 8–13 km altitude over the western Pacific from 1993 to 1999, *Tellus, Ser. B*, *54*, 1–21.

Newell, R. E., et al. (1996), Atmospheric sampling of supertyphoon Mireille with NASA DC-8 Aircraft On September 27, 1991, during PEM-West A, *J. Geophys. Res.*, *101*, 1853–1871.

Peylin, P., P. Bousquet, C. Le Quéré, S. Sitch, P. Friedlingstein, G. McKinley, N. Gruber, P. Rayner, and P. Ciais (2005), Multiple constraints on regional CO_2 flux variations over land and oceans, *Global Biogeochem. Cycles*, *19*, GB1011, doi:10.1029/2003GB002214.

Potter, C. S., J. T. Randerson, C. B. Field, P. A. Matson, P. M. Vitousek, H. A. Mooney, and S. A. Klooster (1993), Terrestrial ecosystem production: A process model based on global satellite and surface data, *Global Biogeochem. Cycles*, *7*, 811–841.

Raper, J. L., M. M. Kleb, D. J. Jacob, D. D. Davis, R. E. Newell, H. E. Fuelberg, R. J. Bendura, J. M. Hoell, and R. J. McNeal (2001), Pacific Exploratory Mission in the Tropical Pacific: PEM-Tropics B, March–April 1999, *J. Geophys. Res.*, *106*, 32,401–32,426.

Rödenbeck, C., S. Houweling, M. Gloor, and M. Heimann (2003), CO_2 flux history 1982–2001 inferred from atmospheric data using a global inversion of atmospheric tracer transport, *Atmos. Chem. Phys.*, *3*, 1919–1964.

Russell, G., and J. Lerner (1981), A new finite-differencing scheme for the tracer transport equation, *J. Appl. Meteorol.*, *20*, 1483–1498.

Sadourny, R., and K. Laval (1984), January and July performance of the LMD general circulation model, in *New Perspectives in Climate Modeling*, edited by A. Berger and C. Nicolis, pp. 173–198, Elsevier, New York.

Smith, W. L., H. M. Woolf, C. M. Hayden, D. Q. Wark, and L. M. McMillin (1979), The TIROS-N Operational Vertical Sounder, *Bull. Am. Meteorol. Soc.*, *60*, 1177–1187.

Thoning, K. W., P. P. Tans, and W. D. Komhyr (1989), Atmospheric carbon dioxide at Mauna Loa Observatory: 2. Analysis of the NOAA GMCC data, 1974–1985, *J. Geophys. Res.*, *94*, 8549–8565.

Tiedtke, M. (1989), A comprehensive mass flux scheme for cumulus parameterization in large-scale models, *Mon. Weather Rev.*, *117*, 1179–1800.

Tiwari, Y. K., M. Gloor, R. J. Engelen, F. Chevallier, C. Rödenbeck, S. Körner, P. Peylin, B. H. Braswell, and M. Heimann (2006), Comparing CO_2 retrieved from Atmospheric Infrared Sounder with model predictions: Implications for constraining surface fluxes and lower-to-upper troposphere transport, *J. Geophys. Res.*, *111*, D17106, doi:10.1029/2005JD006681.

Van der Werf, G. R., J. T. Randerson, G. J. Collatz, and L. Giglio (2003), Carbon emissions from fires in tropical and subtropical ecosystems, *Global Change Biol.*, *9*, 547–562.

C. Brenninkmeijer, Division of Atmospheric Chemistry, Max Planck Institute for Chemistry, D-55020 Mainz, Germany.

F. M. Bréon and P. Ciais, Laboratoire des Sciences du Climat et de l'Environnement, CEA Centre de Saclay, Orme des Merisiers, 91191 Gif sur Yvette, France.

A. Chédin, Laboratoire de Météorologie Dynamique, Ecole Polytechnique, F-91128 Palaiseau, France.

M. Gloor, Earth and Biosphere Institute, University of Leeds, Leeds LS2 9JT, West Yorkshire, UK.

T. Machida, National Institute for Environmental Studies, 16-2 Onogawa, Tsukuba 305-8506, Japan.

P. Peylin, Laboratoire BIOEMCO, Campus INRA/INA PG, bat EGER, 78859 Thiverval-Grignon, France. (philippe.peylin@cea.fr)

S. Serrar, Research Department, Satellite Section, European Center for Medium Range Weather Forecasts, Reading RG2 9AX, UK.

Y. Tiwari, Indian Institute of Tropical Meteorology, Pune Maharashtra, India.

A. Zahn, Institut for Meteorology and Climate Research (IMK), D-76021 Karlsruhe, Germany.